

Alma Mater Studiorum Università di Bologna
Archivio istituzionale della ricerca

Impact of Curved-Blade Impellers on Gas Holdup and Liquid Homogenization Dynamics in Stirred Tanks

This is the final peer-reviewed author's accepted manuscript (postprint) of the following publication:

Published Version:

Zak, A., Moucha, T., Paglianti, A., Montante, G. (2023). Impact of Curved-Blade Impellers on Gas Holdup and Liquid Homogenization Dynamics in Stirred Tanks. CHEMICAL ENGINEERING & TECHNOLOGY, 46(6), 1191-1197 [10.1002/ceat.202200538].

Availability:

This version is available at: <https://hdl.handle.net/11585/926912> since: 2023-11-03

Published:

DOI: <http://doi.org/10.1002/ceat.202200538>

Terms of use:

Some rights reserved. The terms and conditions for the reuse of this version of the manuscript are specified in the publishing policy. For all terms of use and more information see the publisher's website.

This item was downloaded from IRIS Università di Bologna (<https://cris.unibo.it/>).
When citing, please refer to the published version.

(Article begins on next page)

This is the final peer-reviewed accepted manuscript of:

Žák A., Moucha T., Paglianti A., Montante G. Impact of Curved-Blade Impellers on Gas Holdup and Liquid Homogenization Dynamics in Stirred Tanks (2023) Chemical Engineering and Technology, 46 (6), pp. 1191 - 1197.

The final published version is available online at:
<https://doi.org/10.1002/ceat.202200538>

Terms of use:

Some rights reserved. The terms and conditions for the reuse of this version of the manuscript are specified in the publishing policy. For all terms of use and more information see the publisher's website.

This item was downloaded from IRIS Università di Bologna (<https://cris.unibo.it/>)

When citing, please refer to the published version.

Ing. Žák Adrián¹

Prof. Dr. Ing. Tomáš Moucha^{1*}

Prof. Dr. Ing. Alessandro Paglianti²

Prof. Dr. Ing. Giuseppina Montante²

Impact of curved blade impellers on gas hold-up and liquid homogenization dynamics in stirred tanks

Design and optimisation of aerobic fermentation processes in stirred tanks must factor in specific features, such as the formation of gas cavities on the rear of impeller blades and the need for high power input. Here, we investigate the ability of a curved blade impeller to reduce these drawbacks, which are typical of flat blade impellers. The analysis is based on gas hold-up distributions and liquid homogenization dynamics collected by Electrical Resistance Tomography in a pilot scale stirred tank of geometry similar to typical industrial aerated fermenters. A wide range of gas flow rates and impeller speeds in single-impeller and multiple-impeller configurations are considered and the differences arising when a Rushton turbine is replaced with a Bakker turbine are discussed.

Keywords: Curved blade impeller, Electrical resistance tomography, Gas distribution, Liquid homogenization, stirred tank reactor

Author affiliations

¹University of Chemistry and Technology Prague, Department of Chemical Engineering, Prague Technická 5, 166 28, Czech Republic

²University of Bologna, Department of Industrial Chemistry 'Toso Montanari', via Terracini 34, 40131, Bologna, Italy

1. Introduction

Stirred tank reactors belong to the group of mass transfer units which are widely adopted in industrial processes. The vessel development and the efficiency of the gas-liquid system can be determined through key system variables: volumetric mass transfer coefficient, power input and gas hold-up. Gas hold-up is directly connected to gas dispersion. This is mostly obtained through agitation to generate suitable interfacial areas to promote mass and heat transfer [1-3]. Fluid dynamics and mass transfer are strongly related and the mixing characteristic variables such as power number, flow pattern, gas volume fraction, are strongly affected from the impeller type [4]. The most used impellers for gas-liquid mixing are radial flow impellers, although they are the leading energy-consuming component. Energy consumption for agitation can be reduced by combination of axial and radial flow impellers in multiple impeller configurations [5]. Due to the fact that the gas dispersion normally demands impeller power input in a range of 40% - 70% of the whole stirred tank operation, energy-saving and efficient impellers are needed [6].

The Rushton turbine (RT) [7] is the most widespread radial flow impeller used as a standard for decades in agitation process. For this reason, it has been widely investigated so far and found knowledge brings

This item was downloaded from IRIS Università di Bologna (<https://cris.unibo.it/>)

When citing, please refer to the published version.

information about great abilities of agitation and gas dispersion. However, the simple structure of flat blades requires a high power input, gives rise to strong shear force and lead to cavity formation, which reduces mass transfer efficiency in gassed mixing process [8]. Due to these negative impacts, many alternative impeller geometries have been designed to enhance and optimize gas-liquid systems. The main difference between the Rushton turbine and new alternatives are modified blades [1, 9-11]. Many studies proved that the concept of a curved blade impeller is much more effective in the way of power consumption and cavity formation [6, 12-17].

The Bakker turbine (BT), which is characterized by asymmetric concave blades, is a possible alternative to the RT, having the advantages of a power number approximately 2 times lower than the RT in turbulent flow ($BT \approx 2.3$; $RT \approx 5$) [4, 6, 12] and of absence of gas cavities formation in gas-liquid systems. In recent investigations, it was found that gas hold-up and volumetric mass transfer coefficient had relatively small differences with respect to the RT in a measured range of volumetric mass transfer coefficient up to 0.02 1/s [6].

In this work, the Bakker turbine is compared with the Rushton turbine considering the gas hold-up distribution and liquid homogenization dynamics obtained by Electrical Resistance Tomography (ERT) in both single and multiple impeller configurations. ERT is selected, since it is a non-intrusive technique suitable for providing both steady state and transient measurement of the mixture conductivity and it has been already successfully applied for the investigation of gas-liquid equipment, such as bubble columns [18], column reactors [19] stirred tanks [20,21] and in many others multiphase [22-24] and single-phase equipment [25].

2. Material and methods

The experiments were carried out in a pilot-scale stirred tank of inner diameter $T = 0.48$ m, equipped with four standard baffles of thickness equal to $T/10$. Air was injected from the flat bottom of the tank through a ring sparger of diameter equal to 0.09 m set at a clearance from the bottom of 0.09 m and provided with 36 holes of 2 mm in diameter. Demineralized water was used and the ungassed liquid height was equal to T for single impeller configurations and to $2.9 T$ for multiple-impeller configurations. One or three impellers were adopted for agitation. The impellers were the Rushton turbine and the Bakker turbine of standard geometry.

The impeller diameter, D , for the Rushton turbine was 0.19 m. For the Bakker turbine D was 0.195 m, considering nominal diameter, and 0.215 m, considering the swept diameter. Correspondingly, the ratio between the impeller diameter and the vessel diameter, D/T , was equal to 0.4 for RT and 0.44 for BT, based on swept diameter. The clearance of the lower impeller was set at $T/2$, while distance between consecutive impellers was equal to T .

The stirred tank and the instrumentation adopted for the measurements are shown in Figure 1. The ERT measurement system was based on the ITS P2000 instrumentation by Industrial Tomography Systems Ltd. It includes a data acquisition system (DAS), a PC for data acquisition and processing and electrodes, fixed to the vessel wall. The circular electrode arrangement was employed for the voltage measurement. The injected current intensity was set to 15 mA and the frequency to 9600 Hz. To obtain the conductivity tomography on each plane, current was injected on each pair of adjacent electrodes and the voltage difference was measured by the remaining electrodes; the procedure was repeated for all the electrode pairs. For each investigated condition, 1500 frames per plane were collected, with a resolution of 4.4 frames per second. The conductivity maps were reconstructed using the Linear Back Projection algorithm on a square mesh of 20 mm side. Two multiple-impeller and two single impeller arrangements were analysed: a single RT, a single BT, triple RT, 1 BT on the bottom and 2 RT on top. The gas hold-up was measured in single and multiple impeller configurations on two planes (z_1, z_2). The liquid homogenization dynamics were measured in single

This item was downloaded from IRIS Università di Bologna (<https://cris.unibo.it/>)

When citing, please refer to the published version.

impeller configuration on two planes and in multiple impeller configuration on three planes (z_1, z_2, z_3). The locations of the measurement plane are summarized in Table 1.

Measurements were repeated at different impeller rotational speed, N , starting from 50 rpm up to 500 rpm and at gas flow rate, Q_g , of 25, 50, 100 L min⁻¹, as summarized in Table 2. Preliminary measurements of liquid homogenization dynamics in single phase flow were also carried out for comparison. The range of conditions is chosen to cover flooding, loading and fully dispersed flow regimes.

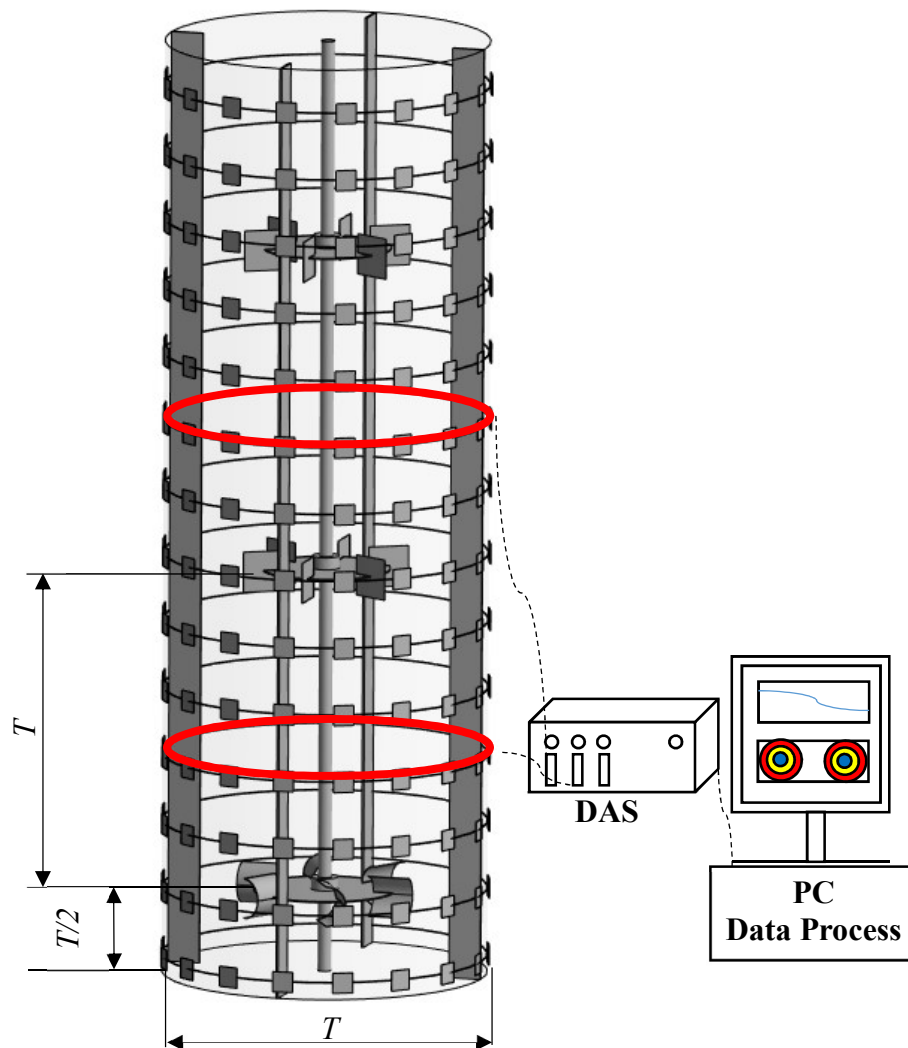


Figure 1 Sketch of the experimental set-up: stirred tank equipped with three impellers. The two horizontal measurement planes are depicted in red.

Table 1 Location of measurement planes

Impeller configuration	Single impeller	Multiple-impeller
Plane, z_1	$0.38 T$	$0.88 T$
Plane, z_2	$0.88 T$	$1.88 T$

This item was downloaded from IRIS Università di Bologna (<https://cris.unibo.it/>)

When citing, please refer to the published version.

Plane, z_3^*	-	2.63 T
----------------	---	--------

*Only for the liquid homogenization measurement

Table 2 Investigated operative conditions

Impeller configuration	Gas flow rate [L min ⁻¹]	Impeller speed [rpm]
Single impeller	0*, 25, 50, 100	50, 100, 200, 300, 400, 500
Multiple-impeller	0*, 25, 50, 100	50, 200, 500

*Only for the liquid homogenization measurement

3. Results and Discussion

3.1. Gas distribution in the liquid phase

The ERT measurements provide the local dimensionless conductivity, c , which is the conductivity of the mixture divided by the conductivity of the ungassed liquid. The characteristic behaviour of gas-liquid distribution in each measurement plane can be investigated by considering the dimensionless conductivity, which varies from 0 (just gas) to 1 (just liquid) and it is related to the gas hold-up. The conductivity of the ungassed liquid was obtained from a preliminary reference measurement with only the liquid phase in the vessel stirred at 50 rpm. The local gas hold-up, α , is evaluated from c , adopting the Maxwell equation, as:

$$\alpha = \frac{2 - 2c}{c + 2} \quad (1)$$

The average gas hold-up on the plane, $\bar{\alpha}$, can be gained as the arithmetic mean of the 316 measurements.

3.1.1 Single-Impeller configuration

In the case of a single impeller configuration, the effect of the flow regime on the gas distribution in the measurement plane set below the impeller can be appreciated analysing Figure S1, shown in the supporting information. In the flooding and complete dispersion regime the effect of the impeller type is weak, while a more uniform distribution in the loading regime was obtained by using a BT.

The effect of the impeller speed at equal gas flow rate is shown in Figure 2, where the average gas hold-up values on the two measurement sections at $Q_G=100$ L min⁻¹ and N in the range 50-500 rpm are reported. As can be observed, at the same impeller speed, on the upper plane (z_2) comparable average gas hold-up with the two impellers is obtained. In the plane below the impeller (z_1), the gas hold-up is very close only at the two lower impeller speed, while for N equal or greater than 200 rpm, agitation with the RT provides higher values.

This item was downloaded from IRIS Università di Bologna (<https://cris.unibo.it/>)

When citing, please refer to the published version.

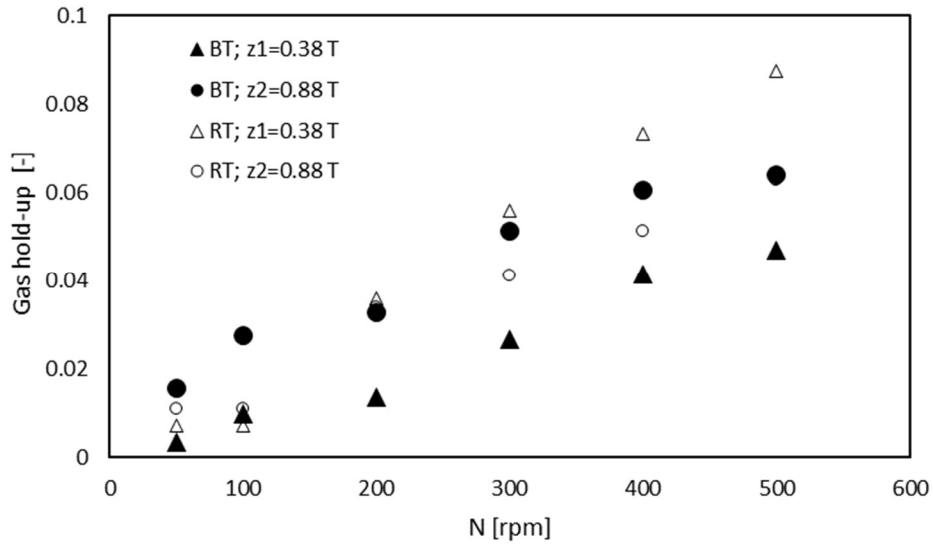


Figure 2 Average gas hold-up below, z_1 , and above, z_2 , the impeller obtained with the RT and the BT.

In order to quantitatively detect the flow regime transition from the ERT data, the Coefficient of Variation of the gas hold-up is calculated as:

$$CoV = \sqrt{\frac{\sum_{i=1}^n \left(\frac{\alpha_i}{\bar{\alpha}} - 1 \right)^2}{n - 1}} \quad (2)$$

where n is the number of cells on the plane, that is equal to 316.

The results shown in Figure 3 summarize the CoV obtained below the impellers at $Q_G=100 \text{ L min}^{-1}$ and variable N .

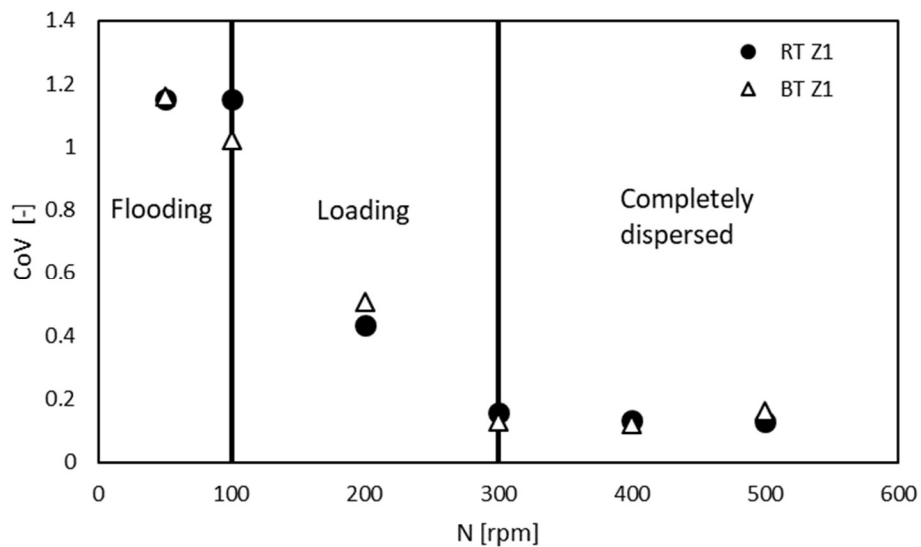


Figure 3 Comparison of CoV vs N for the two impellers. $Q_G=100 \text{ Lmin}^{-1}$.

As can be observed, in the plane below the impeller the experimental data collected with the RT and the BT show that the transition from flooding, characterized by values of the CoV greater than 1, to loading, characterized by intermediate values of CoV, and completely dispersed regime, characterized by values of CoV smaller than 0.15, do not differ significantly. It is worthwhile noticing that, in the case of RT, the impeller speed corresponding to the flow regime transitions identified with the CoV analysis is in agreement with the values obtained from the equations suggested by Nienow [26,27].

Overall, the experimental data of average gas hold-up above the impeller show that BT and RT give comparable results. Moreover, the analysis of the CoV of the gas hold-up measured using BT and RT gives practically the same trend. It should be noticed that the power consumed by the two impeller is different, in fact in single-phase the power number of a RT in turbulent regime is equal to about 5, while the power number of a BT is equal to 2.3 [12]. Being the power number of the two impellers different and the effect of the impeller type on the gas dispersion weak, the results suggest that more efficient mixing is obtained with the lower power number impeller.

3.1.2 Multiple impeller configuration

A comparison of the gas distribution obtained in different regimes with the two different set of multiple impellers is shown in Figure 4. The experimental data relevant to the combination of the Bakker turbine in the lower position and two Rushton Turbines in the upper positions (1BT + 2RT) are presented in Figure 4 A, C and E, while those obtained with the multiple Rushton Turbines (3RT) are shown in Figure 4 B, D and F. In the multiple impeller configuration the attention has been focused on the measurement planes above the lowest impeller, therefore the plane z_1 and z_2 were located at $0.88T$ and $1.88T$ respectively. The local values of the gas hold-up obtained with the two impeller configurations shown in Figure 4 exhibit negligible differences at equal operative conditions, therefore at equal N and Q_G the RT and the BT can be considered equivalent.

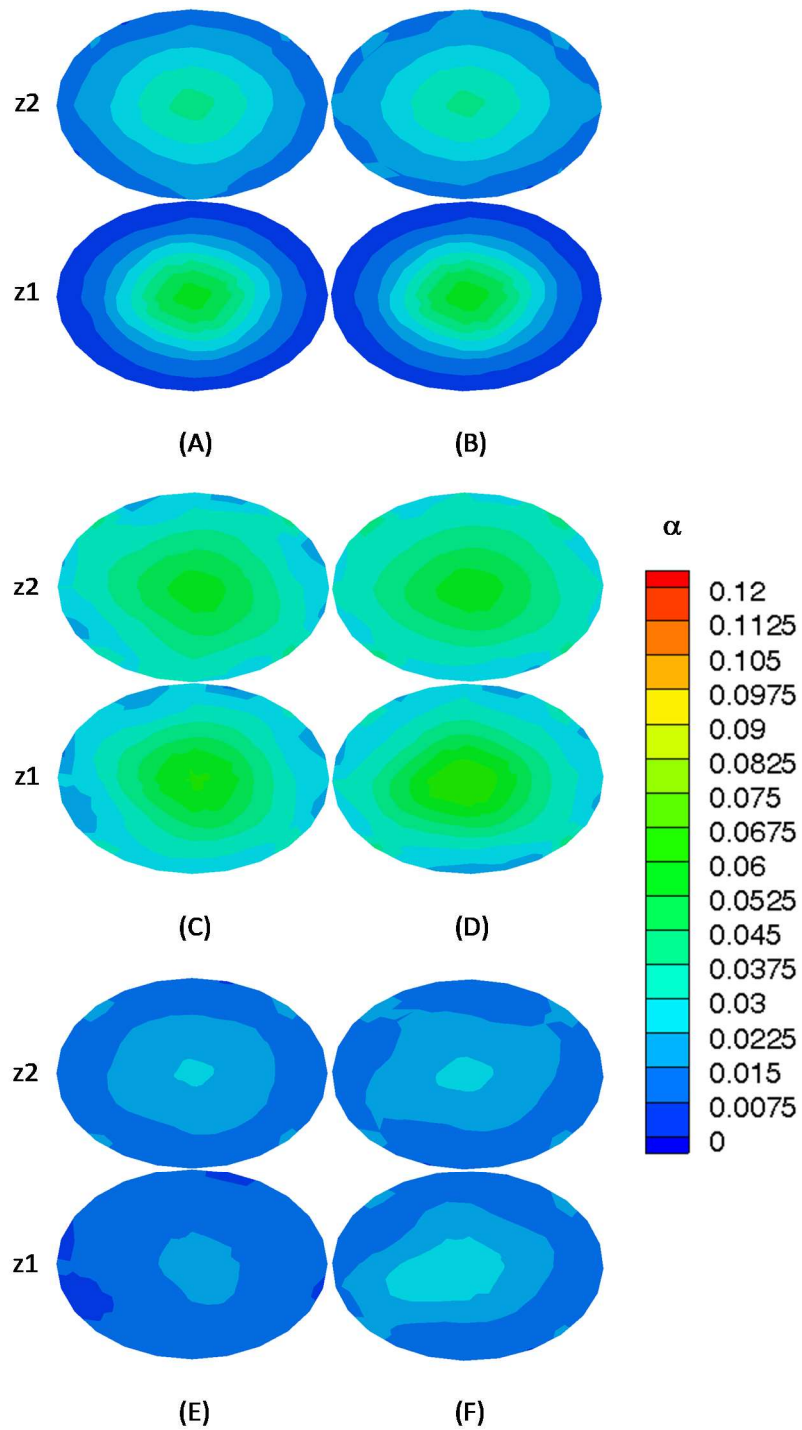


Figure 4 Comparison of gas hold-up distribution obtained with 1BT+2RT (A, C, E) and 3 RT (B, D, F) in multiple impeller configuration. (A, B): flooding regime, $N = 50$ rpm and $Q_G = 100$ L min^{-1} ; (C, D): loading regime, $N = 200$ rpm, $Q_G=100$ L min^{-1} ; (E, F): fully dispersed regime, $N= 200$ rpm, $Q_G=25$ L min^{-1} .

The experimental data shown in Figure 5 allow to compare the effect of the bottom impeller type on the gas hold-up distribution in the vessel volume. As can be observed, on both the measurement planes, which are

This item was downloaded from IRIS Università di Bologna (<https://cris.unibo.it/>)

When citing, please refer to the published version.

located above the bottom impeller, the average gas hold-up obtained with the RT and the BT is approximately the same, apart for the case of the highest value of the impeller speed, for which the hold-up is bigger with the RT. This result agrees with that obtained with single impeller, in that case relevant differences between RT and BT were observed only below the lower impeller. In fact, the experimental data shown in Figure 2 for single impeller configuration evidenced that, above the impeller, the gas hold-up obtained with a RT was comparable to that obtained with a BT. The experimental data obtained with multiple impellers confirm that, in the zone above the lowest impeller, the effects induced by the change of the bottom impeller type, at the same impeller speed, are limited.

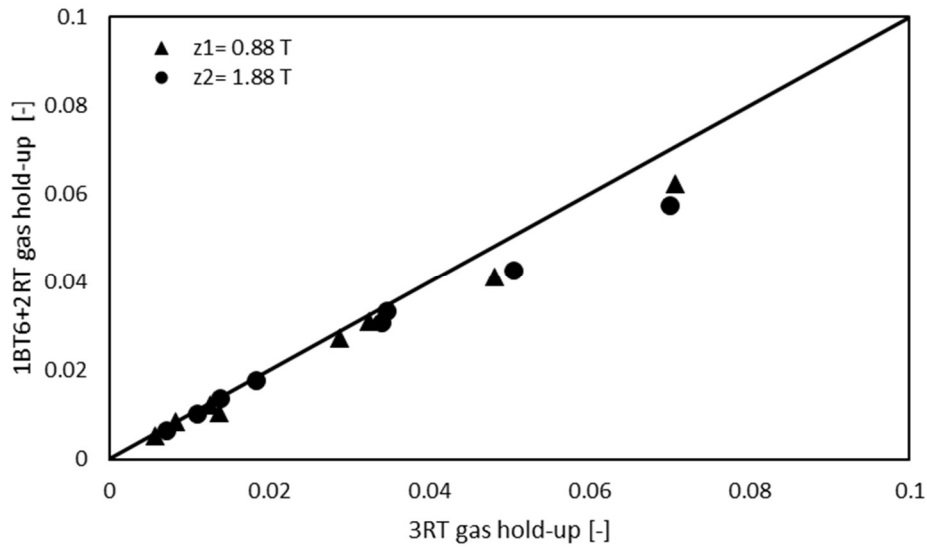


Figure 5 Comparison of average gas hold-up in the two multiple impeller configurations (1BT+ 2RT vs 3RT).

3.2. Liquid phase homogenization

In the following, the homogenization dynamics obtained after the almost instantaneous injection of a small amount (50 mL in the single impeller configuration and 150 mL for the triple impellers) of aqueous NaCl solution (concentration 300 g of NaCl per litre of water) on the free liquid layer is analysed.

The mixing time is obtained from the time trace of the normalized dimensionless conductivity defined as:

$$\chi(t) = \frac{\bar{c}(t) - \bar{c}(0)}{\bar{c}(\infty) - \bar{c}(0)} \quad (3)$$

Where $\bar{c}(t)$ is the average dimensionless conductivity on the measurement plane, $\bar{c}(0)$ is the average dimensionless conductivity measured before the salt addition and $\bar{c}(\infty)$ is the average dimensionless conductivity when the salt solution is fully homogenized.

To assess the dynamics of homogenization obtained with the two impellers, the time required to reach a level of variation within $\pm (1-x)\%$ respect to $\chi(\infty)$, being x the desired degree of homogeneity is adopted. In this work, x is fixed at 0.95, thus determining the so-called t_{95} mixing time. The time evolution of the averaged

This item was downloaded from IRIS Università di Bologna (<https://cris.unibo.it/>)

When citing, please refer to the published version.

dimensionless conductivity was followed on each measurement plane. The mixing time of the vessel has been considered as a maximum value among those obtained in the two/three measurement planes. From triplicate measurements, the maximum relative error of the mixing time estimation was found equal to 9%. The influence of the position of the tracer addition was not specifically investigated.

Typical mixing curves are shown, for the multiple impeller configurations at 50 rpm in single phase flow and with a gas flowrate equal to 25 L min⁻¹, in Figure 6. Experimental data obtained in single-phase flow with a single impeller are shown in Figure S2 of the supporting information.

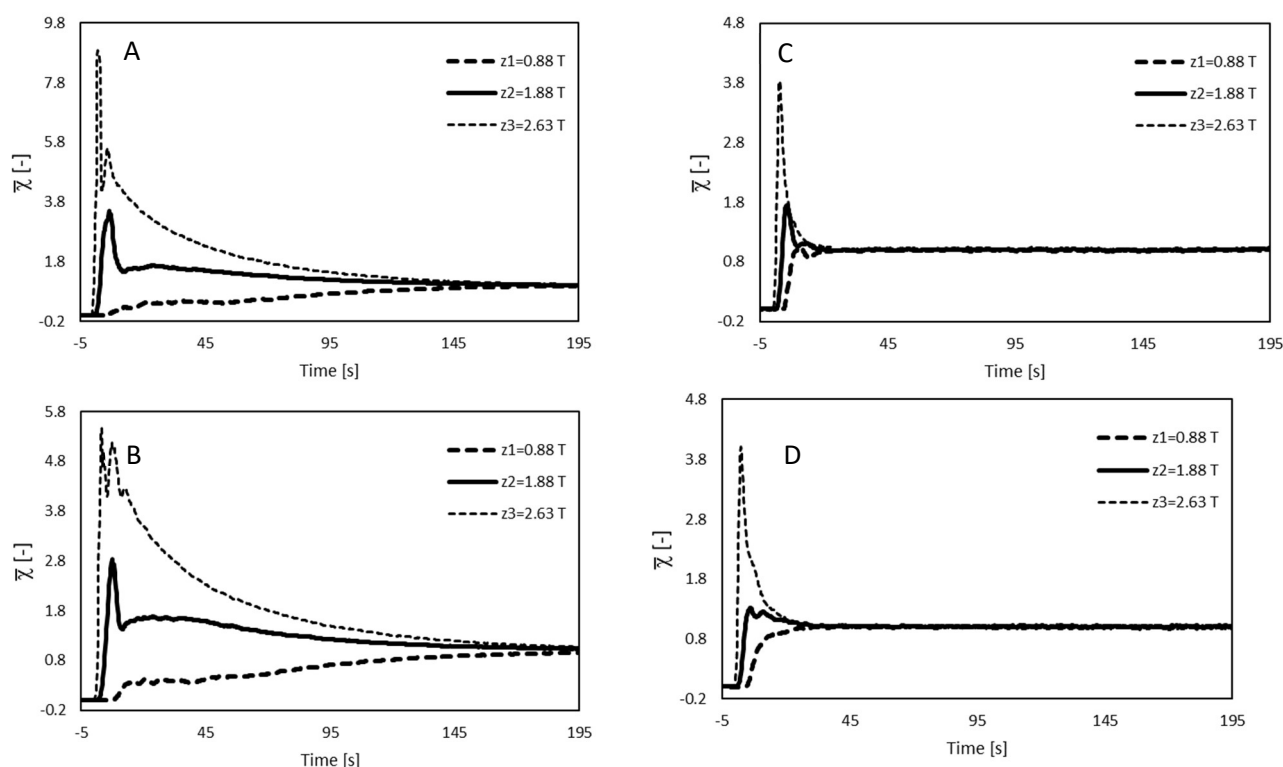


Figure 6 Comparison of the time traces of normalized dimensionless conductivity (A) BT+2RT, N=50 rpm; $Q_G = 0 \text{ L min}^{-1}$ (B) 3RT, N=50 rpm; $Q_G = 0 \text{ L min}^{-1}$, (C) BT+2RT, N=50 rpm; $Q_G = 25 \text{ L min}^{-1}$, (D) 3RT, N=50 rpm; $Q_G = 25 \text{ L min}^{-1}$.

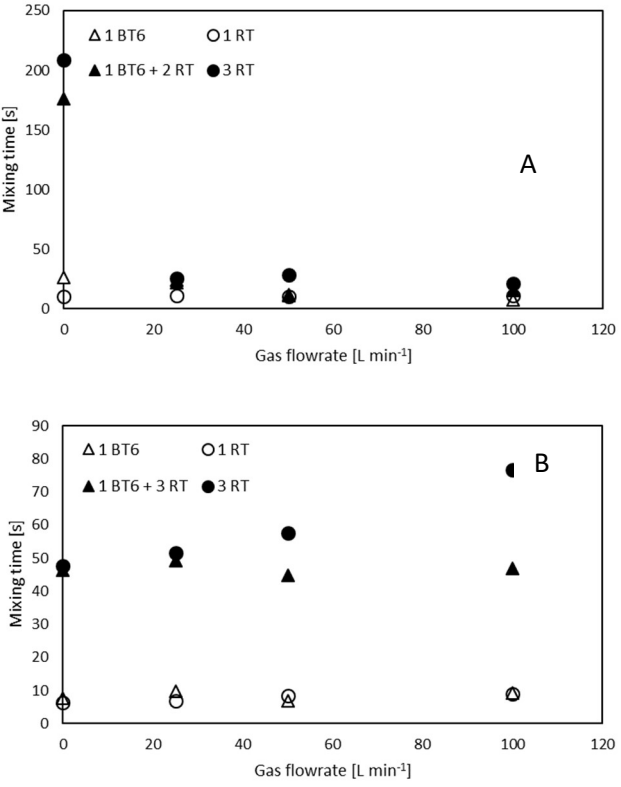
The results show that important differences arise moving from single impeller to multiple impeller systems and from single phase to gas-liquid mixtures. In single phase conditions, both with single RT or single BT, the mixing time is a few tens of seconds (the time traces are reported in the supporting information, Figure S2), while with multiple impellers the characteristic time is close to 200 seconds for both the configurations. As pointed out by Zak et al. [28], the behaviour observed with multiple impellers is due to the zoning effect that limits the mass exchange between adjacent impellers. Moving from single-phase to gas-liquid flow, the negative effect of the compartmentalization of the tank disappears and the mixing time becomes in the order of some tens of seconds, as shown in Figure 7.

The data obtained at N=50, 200 and 500 rpm are shown in Figure 7 (A), (B) and (C) respectively. Mixing time is always longer with multiple impellers than with a single impeller. Obviously, the zoning effect observed

This item was downloaded from IRIS Università di Bologna (<https://cris.unibo.it/>)

When citing, please refer to the published version.

with multiple impeller at 50 rpm is absent for the single impeller configuration. At N=500 rpm the change of the RT with the BT does not induce a clear effect on the time necessary to reach homogenization, while at N=200 rpm, if the gas flowrate is bigger than 40 L min⁻¹, the mixing time is smaller with the BT.



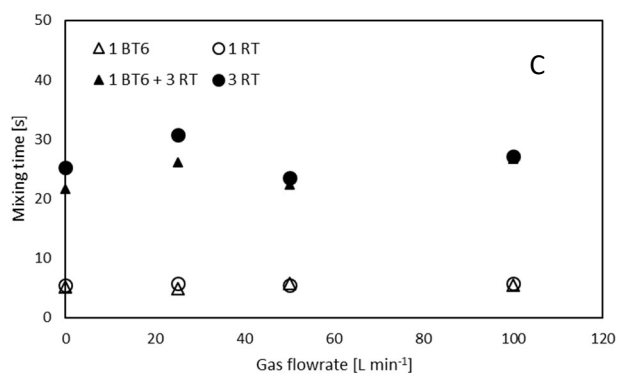


Figure 7 Comparison of mixing times obtained with single and multiple impellers at different gas flowrates. (A) N=50 rpm (B) N=200 rpm, (C) N=500 rpm.

4. Conclusion

The local values of gas hold-up together with the liquid mixing time were investigated with the specific purpose of assessing the difference in gas-liquid mixing performances obtained with the standard Rushton turbine and the asymmetric concave blade design, namely the Bakker turbine, in single and multiple impeller configurations.

The main results are summarized in the following:

- For the single impeller stirred tank, the change of the impeller type from RT to BT, at the same impeller speed, induces small differences both to the gas distribution and to the flow regime transition. Also, the mixing homogenization dynamics, in fully dispersed gas flow regime, exhibit limited difference with the two impellers.
- For multiple impeller system, the effect of the impeller type at equal gas flow rate and impeller speed is weak, since similar gas hold-up distributions are obtained either adopting a RT or a BT in the bottom position. The presence of the gas phase prevents the compartmentalization, observed with the same impeller configuration in single phase conditions.

Overall, considering that similar dispersion of the gas phase and similar mixing time have been obtained using either a RT and a BT at equal gas flow rates and impeller speeds, being the turbulent power number of the BT lower than that of the RT, the BT is more energetically efficient for gas-liquid mixing.

Supporting Information

Supporting Information for this article can be found under [Link provided by Wiley].

Acknowledgment

Adrian Zak wishes to express his special gratitude to the Specific university research – grant No A1_FCHI_2022_005 for supporting financially his stay at the University of Bologna.

Symbols used

This item was downloaded from IRIS Università di Bologna (<https://cris.unibo.it/>)

When citing, please refer to the published version.

Latin letter

c [-]	Dimensionless conductivity
D [m]	Impeller diameter
N [s ⁻¹]	Impeller rotational speed
t_{95} [s]	Mixing time
T [m]	Diameter of the vessel
Q_g [m ³ s ⁻¹]	Gas flow rate
z_i [m]	Height of the planes (i = 1, 2, 3)

Greek letters

α [-]	Volume fraction of the dispersed material/local gas hold-up
$\bar{\alpha}$ [-]	Average gas hold-up on plane
χ [-]	Normalized dimensionless conductivity

Abbreviations

BT	Bakker Turbine
CoV	Coefficient of Variation
ERT	Electrical resistance tomography
RT	Rushton Turbine

References

1. A. Bakker, J.M. Smith, K.J. Myers, *Chem. Eng.* **1994**, 101(12) 98-102.
2. S. Hiraoka, Y. Kato, Y. Tada, N. Ozaki, Y. Murakami, Y.S. Lee, *Chem. Eng. Res. Des.* **2001**, 79 (8) 805-810. <https://doi.org/10.1205/02638760152721613>
3. A.M. O'Rourke, P.F. MacLoughlin, *Chem. Eng. Process.* **2005**, 44 (8) 885-894. <https://doi.org/10.1016/j.cep.2004.10.001>
4. K. Yapici, B. Karasozen, M. Schäfer, Y. Uludag, *Chem. Eng. Process.* **2008**, 47 (8) 1340-1349. <https://doi.org/10.1016/j.cep.2007.05.002>
5. P.R. Gogate, A.A.C.M. Beenackers, A.B. Pandit, *Biochem. Eng. J.* **2000**, 6 (2) 109-144. [https://doi.org/10.1016/S1369-703X\(00\)00081-4](https://doi.org/10.1016/S1369-703X(00)00081-4)
6. Z. Zheng, D. Sun, J. Li, X. Zhan, M. Gao, *Chem. Eng. Res. Des.* **2018**, 130 199-207. <https://doi.org/10.1016/j.cherd.2017.12.021>
7. J.H. Rushton, *Chem. Eng. Prog.* **2050**, 46 395-404.
8. K. Van't Riet, J.M. Smith, *Chem. Eng. Sci.* **1975**, 30 (9) 1093-1105. [https://doi.org/10.1016/0009-2509\(75\)87012-6](https://doi.org/10.1016/0009-2509(75)87012-6)
9. K. van't Riet, J.M. Boom, J.M. Smith, *Trans. Inst. Chem. Eng.* **1976**, 54 (2) 124-131.
10. M.M.C.G. Warmoeskerken, J.M. Smith, *Chem. Eng. Res. Des.* **1989**, 67 193-198.
11. S.C.P. Orvalho, J.M.T. Vasconcelos, S.S. Alves, in *Proc. of 10th European Conference on Mixing* (Eds H.E.A. van den Akker J.J. Derksen) Elsevier Science, Amsterdam **2000**, 461-468. <https://doi.org/10.1016/B978-044450476-0/50058-3>
12. D. Pinelli, A. Bakker, K.J. Myers, M.F. Reeder, J. Fasano, F. Magelli, *Chem. Eng. Res. Des.* **2003**, 81 (4) 448-454. <https://doi.org/10.1205/026387603765173709>
13. R. Afshar Ghotli, A.A. Abdul Raman, S. Ibrahim, *Measurement*, **2016**, 91 440-450. <https://doi.org/10.1016/j.measurement.2016.04.044>
14. T.T. Devi, B. Kumar, *Eng. Sci. Technol. Int. J.* **2017**, 20 (2) 730-737. <https://doi.org/10.1016/j.jestch.2016.11.005>

This item was downloaded from IRIS Università di Bologna (<https://cris.unibo.it/>)

When citing, please refer to the published version.

15. R. Afshar Ghotli, A.R. Abdul Aziz, S. Ibrahim, S. Baroutian, A. Arami-Niya, *J. Taiwan Inst. Chem. Eng.* **2013**, *44* (2) 192-201. <https://doi.org/10.1016/j.jtice.2012.10.01016>.
16. H. Ameer, *Chem. Eng. Process.* **2020**, *154* 108009. <https://doi.org/10.1016/j.cep.2020.108009>
17. H. Majirova, D. Pinelli, V. Machon, F. Magelli, *Chem. Eng. Technol.* **2004**, *27*(3) 304-309. <https://doi.org/10.1002/ceat.200401989>
18. M.A. Bennett, R.M. West, S.P. Luke, X. Jia, R.A. Williams, *Chem. Eng. Sci.* **1999**, *54* (21) 5003-5012. [https://doi.org/10.1016/S0009-2509\(99\)00224-9](https://doi.org/10.1016/S0009-2509(99)00224-9)
19. H.Jin, M. Wang, R.A. Williams, *Chem. Eng. J.* **2007**, *130* (2) 179- 185. <https://doi.org/10.1016/j.cej.2006.08.032>
20. G. Montante, A. Paglianti, *Chem. Eng. J.* **2015**, *279* 648-658. <https://doi.org/10.1016/j.cej.2015.05.058>
21. M.Wang, F.J. Dickin, R. Mann, *Chem. Eng. Commun.* **1999**, *175* (1) 49-70. <https://doi.org/10.1080/00986449908912139>
22. S. Hosseini, D. Patel, F. Ein-Mozaffari, M. Mehrvar, *Chem. Eng. Sci.* **2010**, *65* (4) 1374-1384. <https://doi.org/10.1016/j.ces.2009.10.007>
23. G. Montante, C. Carletti, F. Maluta, A. Paglianti, *Chem. Eng. Technol.* **2019**, *42*(8) 1627-1634. <https://doi.org/10.1002/ceat.201800726>
24. A. Paglianti, C. Carletti, G. Montante, *Chem. Eng. Technol.* **2017**, *40*(5) 862-869. <https://doi.org/10.1002/ceat.201600595>
25. M.Sharifi, B. Young, *Chem. Eng. Res. Des.* **2013**, *91* (9) 1625-1645. <https://doi.org/10.1016/j.cherd.2013.05.026>
26. A.W. Nienow, M.M.C.G. Warmoeskerken, J.M. Smith, M. Konno, in Proceedings of the Fifth Eur. Conf. Mix., BHRA Fluid Engineering, Wurzburg, Germany, 1985, 143–154.
27. A.W. Nienow, D.J. Wisdom, J.C. Middleton, in Proceedings of the Second Eur. Conf. Mix., BHRA Fluid Engineering, Mons, BE, 1977, F1-1–F1-16.
28. A.Zak, F. Alberini, F. Maluta, T. Moucha, G. Montante, A. Paglianti, *Chem. Eng. Res. Des.* **2022**, *184* 501-512. <https://doi.org/10.1016/j.cherd.2022.06.021>

Table and Figure captions

Figure 8 Sketch of the experimental set-up: stirred tank equipped with three impellers. The two horizontal measurement planes are depicted in red.

Figure 9 Average gas hold-up below, z_1 , and above, z_2 , the impeller with the RT and the BT.

Figure 10 Comparison of CoV vs N for the two impellers. $Q_G=100 \text{ L min}^{-1}$.

Figure 11 Comparison of gas hold-up distribution obtained with 1BT+2RT (A, C, E) and 3 RT (B, D, F) in multiple impeller configuration. (A, B): flooding regime, $N = 50 \text{ rpm}$ and $Q_G = 100 \text{ L min}^{-1}$; (C, D): loading regime, $N = 200 \text{ rpm}$, $Q_G=100 \text{ L min}^{-1}$; (E, F): fully dispersed regime, $N= 200 \text{ rpm}$, $Q_G=25 \text{ L min}^{-1}$.

Figure 12 Comparison of average gas hold-up in the two multiple impeller configurations (1BT+ 2RT vs 3RT).

Figure 13 Comparison of the time traces of normalized dimensionless conductivity (A) BT+2RT, $N=50 \text{ rpm}$; $Q_G = 0 \text{ L min}^{-1}$ (B) 3RT, $N=50 \text{ rpm}$; $Q_G = 0 \text{ L min}^{-1}$, (C) BT+2RT, $N=50 \text{ rpm}$; $Q_G = 25 \text{ L min}^{-1}$, (D) 3RT, $N=50 \text{ rpm}$; $Q_G = 25 \text{ L min}^{-1}$.

Figure 14 Comparison of mixing times obtained with single and multiple impellers at different gas flowrates. (A) $N=50 \text{ rpm}$ (B) $N=200 \text{ rpm}$, (C) $N=500 \text{ rpm}$.

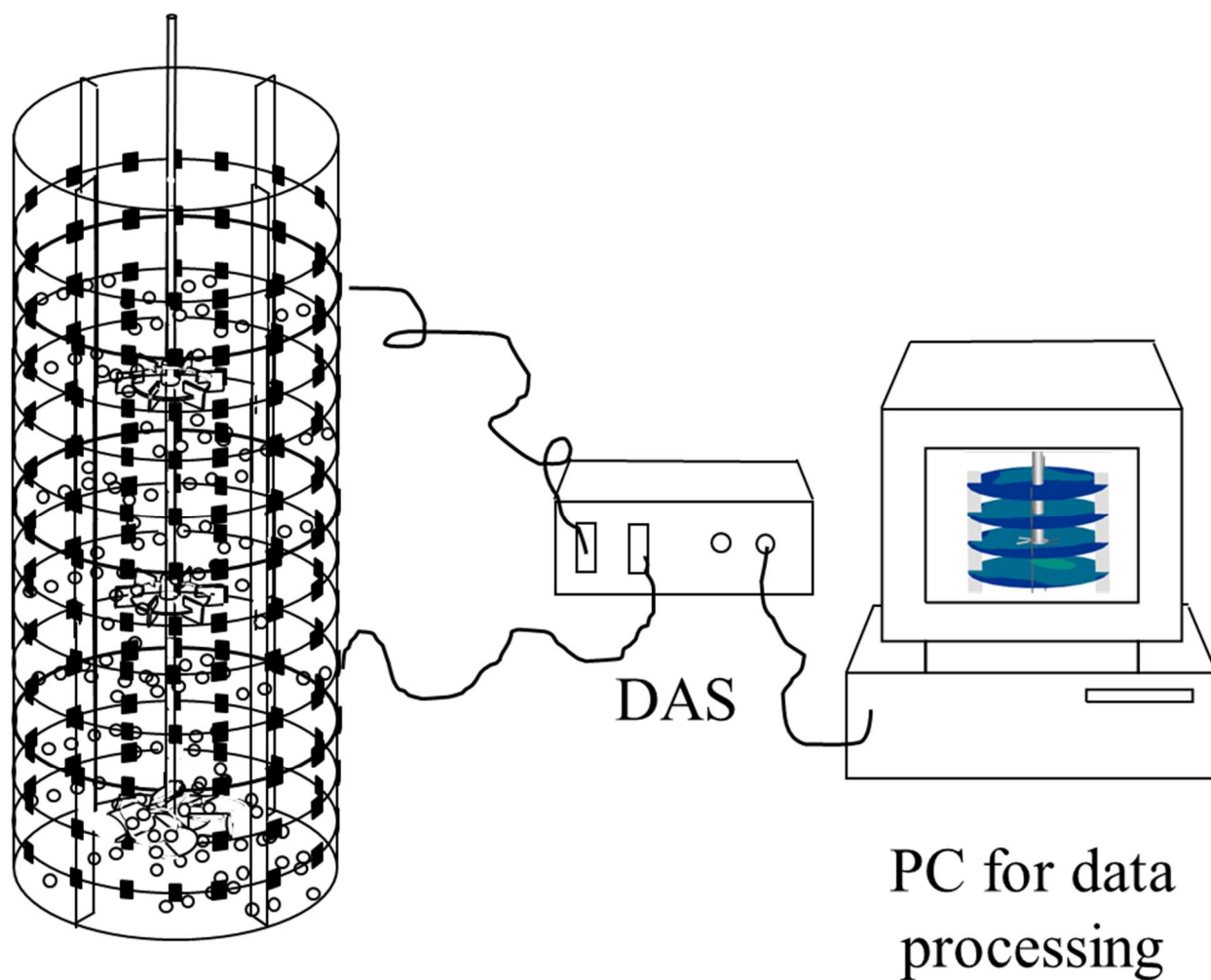
This item was downloaded from IRIS Università di Bologna (<https://cris.unibo.it/>)

When citing, please refer to the published version.

Table 2 Location of measurement planes

Table 3 Measured conditions of each impeller configuration

TOC



This item was downloaded from IRIS Università di Bologna (<https://cris.unibo.it/>)

When citing, please refer to the published version.